Structural Consequences of the Replacement of Glycine M203 with Aspartic Acid in the Reaction Center from *Rhodobacter sphaeroides*[†,‡]

Paul K. Fyfe,[§,||] Justin P. Ridge,[§,⊥] Katherine E. McAuley,[@,#,$] Richard J. Cogdell,[@] Neil W. Isaacs,[#] and Michael R. Jones*[,§,||]

Krebs Institute for Biomolecular Research and Robert Hill Institute for Photosynthesis, Department of Molecular Biology and Biotechnology, University of Sheffield, Western Bank, Sheffield S10 2UH, United Kingdom, and Division of Biochemistry and Molecular Biology and Department of Chemistry, University of Glasgow, Glasgow G12 8QQ, United Kingdom

Received October 28, 1999; Revised Manuscript Received March 7, 2000

ABSTRACT: Reaction centers with the double mutation Phe M197 to Arg and Gly M203 to Asp (FM197R/GM203D) have been crystallized from an antenna-deficient strain of *Rhodobacter sphaeroides*, and the structure has been determined at 2.7 Å resolution. Unlike in reaction centers with a single FM197R mutation, the Arg M197 residue in the FM197R/GM203D reaction center adopts a position similar to that of the native Phe residue in the wild-type reaction center. Asp M203 is packed in such a way that the γ-carboxy group interacts with the backbone carbonyl of Arg M197. The Asp M203 residue takes up part of the volume that is occupied in the wild-type reaction center by a water molecule. This water has been proposed to form a hydrogen bond interaction with the 9-keto carbonyl group of the active branch accessory bacteriochlorophyll, particularly when the primary donor bacteriochlorophylls are oxidized. The GM203D mutation therefore appears to remove the possibility of this hydrogen bond interaction by exclusion of this water molecule, as well as altering the local dielectric environment of the 9-keto carbonyl group. We examine whether the observed structural changes can provide new or alternative explanations for the absorbance and electron-transfer properties of reaction centers with the FM197R and GM203D mutations.

In purple photosynthetic bacteria such as *Rhodobacter* (*Rb.*) *sphaeroides*, the conversion of light energy into electrochemical potential energy takes place in membrane-bound pigment−protein complexes termed reaction centers. The *Rb. sphaeroides* reaction center consists of three subunits, termed H, L, and M, that encase 10 cofactors. These are four molecules of bacteriochlorophyll (BChl),[1] two molecules of bacteriopheophytin (BPhe), two molecules of ubiquinone, a single photoprotective carotenoid, and a non-heme iron atom. The BChl, BPhe, and ubiquinone cofactors are arranged in two membrane-spanning branches around an axis of pseudo-2-fold symmetry (*1*−*7*). Only the branch of cofactors most closely associated with the L subunit is used for light-driven picosecond time scale transmembrane electron transfer (termed the "active" branch, with cofactors most closely associated with the M subunit being termed the "inactive" branch) (*8*−*10*). The primary donor of electrons (P) is a pair of excitonically coupled BChl molecules that straddle the symmetry axis close to the periplasmic face of the protein. On excitation of P, either by direct absorption of a photon or by the transfer of excitation energy from the other pigments of the photosynthetic apparatus, the first singlet excited state of P (P*) drives the reduction of, sequentially, a monomeric BChl (B_L) and a BPhe (H_L) on the active branch of cofactors, forming the so-called $P^+H_L^-$ radical pair state via the intermediate state $P^+B_L^-$ (*11*−*14*). The P* state has a lifetime of 3−5 ps at room temperature (*8*−*10*). The electron is then passed on from H_L to the Q_A ubiquinone in approximately 200 ps at room temperature, completing light-driven transmembrane electron transfer (*8*−*10*).

In a recent report, the X-ray crystal structure of a reaction center with a Phe to Arg mutation at residue M197 (FM197R) was described (*15*). The FM197R mutation causes a 78 mV increase in the midpoint potential of the P/P^+ redox couple (*16*), and X-ray crystallography has shown that this modulation probably occurs through the donation of a hydrogen bond to the 2-acetyl carbonyl group of the M-side P BChl (P_M) by a water molecule (*15*). The Arg residue at M197 does not adopt the "buried" conformation of the wild-

[†] This work was supported by the Biotechnology and Biological Sciences Research Council of the United Kingdom and Wellcome Trust Grant 043492.

[‡] The coordinates of the structure of the FM197R/GM203D reaction center have been deposited in the RCSB data bank under accession number 1E14.

* To whom correspondence should be addressed: Department of Biochemistry, School of Medical Sciences, University of Bristol, University Walk, Bristol BS8 1TD, United Kingdom. Telephone: 44-117-9287571. Fax: 44-117-9288274. E-mail: m.r.jones@bristol.ac.uk.

[§] University of Sheffield.

[||] Present address: Department of Biochemistry, School of Medical Sciences, University of Bristol, University Walk, Bristol BS8 1TD, United Kingdom.

[⊥] Present address: Department of Microbiology, University of Queensland, St. Lucia, Brisbane, QLD 4072, Australia.

[@] Division of Biochemistry and Molecular Biology, University of Glasgow.

[#] Department of Chemistry, University of Glasgow.

[$] Present address: Department of Chemistry, University of York, Heslington, York YO10 5DD, United Kingdom.

[1] Abbreviations: BChl, bacteriochlorophyll; BPhe, bacteriopheophytin; LDAO, lauryldimethylamine oxide; P, primary donor; *Rb*, *Rhodobacter*.

10.1021/bi9925017 CCC: $19.00 © 2000 American Chemical Society
Published on Web 05/02/2000

type Phe residue, pointing toward the 2-acetyl carbonyl group of the P_M BChl, but rather adopts a "flipped-out" conformation, interacting with Asp L155 at the surface of the reaction center and creating a small cavity in the interior of the protein (*15*). This cavity contains a water molecule that is within hydrogen-bonding distance of the 2-acetyl carbonyl group of P_M BChl (*15*).

In a second recent report, the low-temperature (12 K) absorbance properties of the membrane-bound FM197R reaction center were described (*17*). The mutation causes a change in absorbance in the 800 nm region that results in the resolution of two distinct peaks at 801 and 811 nm, rather than the single band at 804 nm and a pronounced shoulder on the red side of the band that is observed in the spectrum of the wild-type reaction center at this temperature (*17*). This effect, which is probably due to an increase in the energy of the Q_y transition of the B_L monomeric BChl, is even more pronounced if the FM197R mutation is made in tandem with a mutation of Gly M203 to Asp (GM203D). The 12 K absorbance spectrum of the membrane-bound double FM197R/GM203D mutant reaction center exhibits discrete peaks at 799 and 814 nm (*17*). This finding is consistent with an earlier report of the 20 K absorbance spectrum of purified reaction centers containing the GM203D single mutation, which showed two absorbance bands separated by 15 nm in this region (*18*). This Gly to Asp mutation is of particular interest because, when the analogous GM201D mutation is made in tandem with the mutation LM212H near the L-side BPhe in the *Rb. capsulatus* reaction center, it perturbs L-branch electron transfer in such a way that a small amount of M-branch electron transfer is observable (*19*). The strong inference from the spectroscopic properties of the GM203D reaction center is that this effect is due, at least in part, to a change in the properties of the B_L BChl (*17*, *18*, *20*).

In this report, we describe the X-ray crystal structure of the FM197R/GM203D reaction center, determined at a resolution of 2.7 Å. The changes in structure observed throw new light on the effect of the GM203D mutation on electron transfer in the reaction center. Findings from the crystal structure also give information on how protein−cofactor interactions may affect the absorbance properties of the P BChls, and on the packing of highly polar amino acids into the hydrophobic interior of the protein.

MATERIALS AND METHODS

Biological Material. The construction of reaction centers with the mutations FM197R, GM203D, and FM197R/GM203D was described recently (*17*). The mutant strains lack the LH1 and LH2 antenna complexes, and contain the mutant reaction center as the sole pigment−protein complex. The crystallographic data obtained in this study were compared with structural models derived from X-ray data for the wild-type reaction center at 2.6 Å resolution (*15*), for the FM197R reaction center at 2.6 Å resolution (*21*), for the FM197R/YM177F reaction center at 2.55 Å resolution (*15*), and for the FM197R/WM115F reaction center at 2.3 Å resolution (*22*). The structures of the latter two reaction centers in the vicinity of residue FM197R are essentially identical to that of the single FM197R mutant reaction center. The mutations YM177F and WM115F both concern residues in the carotenoid binding pocket, and have no apparent effect on the structure of the reaction center outside the immediate vicinity of the mutation site (*21*, *22*). The spectroscopic properties of the FM197R, FM197R/YM177F, and FM197R/WM115F reaction centers are essentially identical (*21*). Therefore, for the purposes of this report, these three reaction centers are regarded as complexes with a single FM197R mutation. The structure of the FM197R/YM177F reaction center has been reported (*15*), and the coordinates have been deposited in the Protein Data Bank under accession code 1MPS. Limited information on the structures of the FM197R and FM197R/WM115F reaction centers has also been reported (*21*, *22*), and a more detailed report is being prepared.

Table 1: Absorbance Maxima at 77 K in the Spectra of Membrane-Bound Reaction Centers

	H Q_y band (nm)	high-energy component of the B Q_y band (nm)	low-energy component of the B Q_y band (nm)	P Q_y band (nm)
wild-type	758	804	814[a]	893
FM197R	758	802	814	878
GM203D	757	800	813	891
FM197R/GM203D	757	799	814	868

[a] In the spectrum of the wild-type reaction center, this band is a shoulder on the main band at 804 nm rather than a discrete component.

Procedures used for cell growth, membrane preparation, and purification and crystallization of the FM197R/GM203D reaction center were as described previously (*15*) with the exception that 1,4-dioxane was omitted from the crystallization solution. Large crystals appeared within 1−4 weeks. As in our previous studies (*15*, *21*, *22*), the crystals of the FM197R/GM203D reaction center belonged to space group $P3_121$; the crystals had the following unit cell dimensions: $a = b = 140.0$ Å, $c = 184.6$ Å, $\alpha = \beta = 90°$, and $\gamma = 120°$.

Crystallography. X-ray diffraction data were collected at 100 K at the EMBL BW7B beamline at HASYLAB/DESY (Hamburg, Germany). Cryoprotection of the crystal to be used for data collection was achieved by stepwise addition and subsequent removal of aliquots of cryoprotectant solution to the crystal in mother liquor. The cryoprotectant solution was 10% (*R*,*R*)-2,3-butanediol, 3.5% heptane-1,2,3-triol, 1.4 M potassium phosphate, and 0.45% LDAO (pH 8.0). Two cryocooled crystals with approximate dimensions of 0.6 mm × 0.3 mm × 0.3 mm were used for the collection of the diffraction data. The data were collected on a MAR345 image plate and processed using the Denzo and Scalepack packages (*23*). Data collection and refinement statistics are shown in Table 2.

Rigid-body refinement was performed using XPLOR 3.1 (*24*) using as a starting model the coordinates of the wild-type reaction center (*15*) with residues M190−M206 and all solvent molecules omitted. The missing residues were rebuilt in O (*25*), and restrained maximum likelihood refinement in REFMAC (*26*) was then carried out.

In Figure 2, structures were illustrated using the programs Molscript (*27*), Raster3D (*28*), and O (*25*).

Spectroscopy. The 77 K absorbance spectra were recorded on a Beckman DU640 spectrophotometer using an Oxford Instruments DN1704 liquid nitrogen cryostat. Reaction center-only, antenna-deficient membranes were diluted in 20

Table 2: Crystallographic Statistics for Data Collection and Refinement

	FM197R/GM203D reaction center
collection statistics	
no. of unique reflections	53587
completeness (%)[a]	92.6 (83.0)
multiplicity	2.8 (2.4)
R_{merge}[a,b] (%)	8.1 (38.8)
refinement statistics	
resolution range (Å)	30.0−2.7
R factor[c] (%)	22.6
R_{free}[d] (%)	26.8
average B factor for buried atoms[e] (Å^2)	42.6
geometry	
rmsd from ideality	
bonds (Å)	0.011
angles (deg)	2.3
residues in the Ramachandran plot[f] (%)	
most favored areas	89.3
additional allowed areas	10.3
generously allowed areas	0.4
disallowed areas	0.0
coordinate error[g] (Å)	0.36
model	
no. of protein residues	833
no. of pigments	4 Bchl, 2 Bphe, 2 Ubi, 1 Spo, 1 Fe
no. of waters	112
no. of detergents	3
no. of lipids	1

[a] Figures within parentheses refer to the statistics for the outer resolution shell (2.7−2.76 Å). [b] $R_{merge} = \Sigma_h\Sigma_i|\langle I(h)\rangle - I(h)_i|/\Sigma_h\Sigma_i I(h)_i$, where $I(h)$ is the intensity of reflection h, Σ_h is the sum over all reflections, and Σ_i is the sum over all i measurements of reflection h. [c] The R factor is defined by $\Sigma||F_o| - |F_c||/\Sigma|F_o|$. [d] R_{free} was calculated with 5% reflections, selected randomly (*39*). [e] Calculated with the program WHATCHECK (*40*). [f] The Ramachandran plot was produced with Procheck version 3.0 (*41*). [g] Coordinate error was estimated with Cruickshank's DPI (*42*).

mM Tris buffer (pH 8.0), supplemented with sodium ascorbate (10 mM) and phenazine methosulfate (20 μM) to ensure full reduction of the P Q_y band, and gently mixed 40:60 (v:v) with glycerol.

RESULTS AND DISCUSSION

Absorbance Spectra. The 77 K absorbance spectra were recorded for reaction center-only membranes from control strain RCO1 (*29*), which has wild-type reaction centers, and the FM197R, GM203D, and FM197R/GM203D mutant strains (Figure 1). In the spectrum of the wild-type reaction center, the band at 893 nm is attributable to the low-energy exciton component of the Q_y transition of the P BChls (P Q_y band), the band at 758 nm is attributable to the Q_y transition of the two reaction center BPhes (H Q_y band), and the asymmetric band at 804 nm is attributable to the Q_y transitions of the monomeric BChls together with the high-energy exciton component of the Q_y transition of P (B Q_y band) (*10*). The B Q_y band had a main peak at 804 nm, which is usually attributed to the Q_y transition of the B_L BChl, and a shoulder on the red side at approximately 814 nm which is usually attributed to the Q_y transition of the B_M BChl and/or the high-energy exciton component of the Q_y transition of P (*10*).

The spectrum of the membrane-bound FM197R reaction center is also shown in Figure 1. The spectroscopic properties

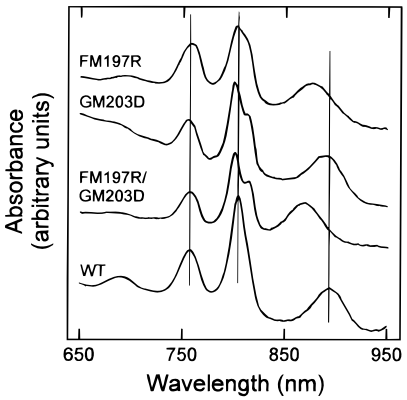

FIGURE 1: The 77 K absorbance spectra of membrane-bound reaction centers. The vertical lines indicate the maxima of the H, B, and P Q_y bands (left to right) in the spectrum of the wild-type reaction center.

of the FM197R reaction center at 12 K have been reported (*17*), and discussed in light of the X-ray crystal structure of this complex (*15*). In accord with these studies, the 77 K absorbance spectrum of the membrane-bound FM197R reaction center exhibited a 15 nm blue shift of the P Q_y band, and a 2 nm blue shift of the main peak of the B Q_y band to 802 nm (Figure 1 and Table 1). The spectrum of the membrane-bound GM203D reaction center exhibited an ∼1 nm blue shift of the H Q_y band, and a ∼2 nm blue shift of the P Q_y band relative to the spectrum of the wild-type reaction center (Figure 1 and Table 1). In the B Q_y region, there was a 4 nm blue shift of the main peak to 800 nm, with the result that the shoulder on the red side of the band was resolved as a discrete peak at 813 nm (Figure 1). This result was in good agreement with published data for the purified GM203D reaction center, which reported two peaks separated by 15 nm in the B Q_y region at 20 K (*18*). In both the FM197R and GM203D reaction centers, the simplest interpretation of the improved resolution of the contributions to the B Q_y band was a blue shift of the main peak (Table 1), indicating effects of both mutations on the Q_y transition of B_L.

The spectrum of the FM197R/GM203D reaction center exhibited a 25 nm blue shift of the P Q_y band, larger than the 15 nm blue shift seen for the FM197R reaction center (Figure 1 and Table 1). This 10 nm difference did not simply arise from an additive effect of the two single mutations, as the GM203D mutation blue shifted the P Q_y band by only 2 nm relative to that of the wild type (see above). The spectrum of the FM197R/GM203D reaction center in the H and B Q_y regions was similar to that of the GM203D single mutant. The H Q_y band exhibited an ∼1 nm blue shift, and the B Q_y band exhibited a main peak at 799 nm, blue shifted 5 nm from the position in the spectrum of the wild-type reaction center, allowing the shoulder on the red side of this band to be resolved as a discrete peak at 814 nm. Again, the simplest interpretation of this change is an increase in the energy of the Q_y transition of B_L.

To summarize, therefore, the main effect of the GM203D mutation was to enhance the asymmetry of the B Q_y band, probably by increasing the energy of the Q_y transition of B_L, and similar effects were seen in the single and double mutant with this change. The FM197R mutation had a smaller effect on the asymmetry of this band, but its main

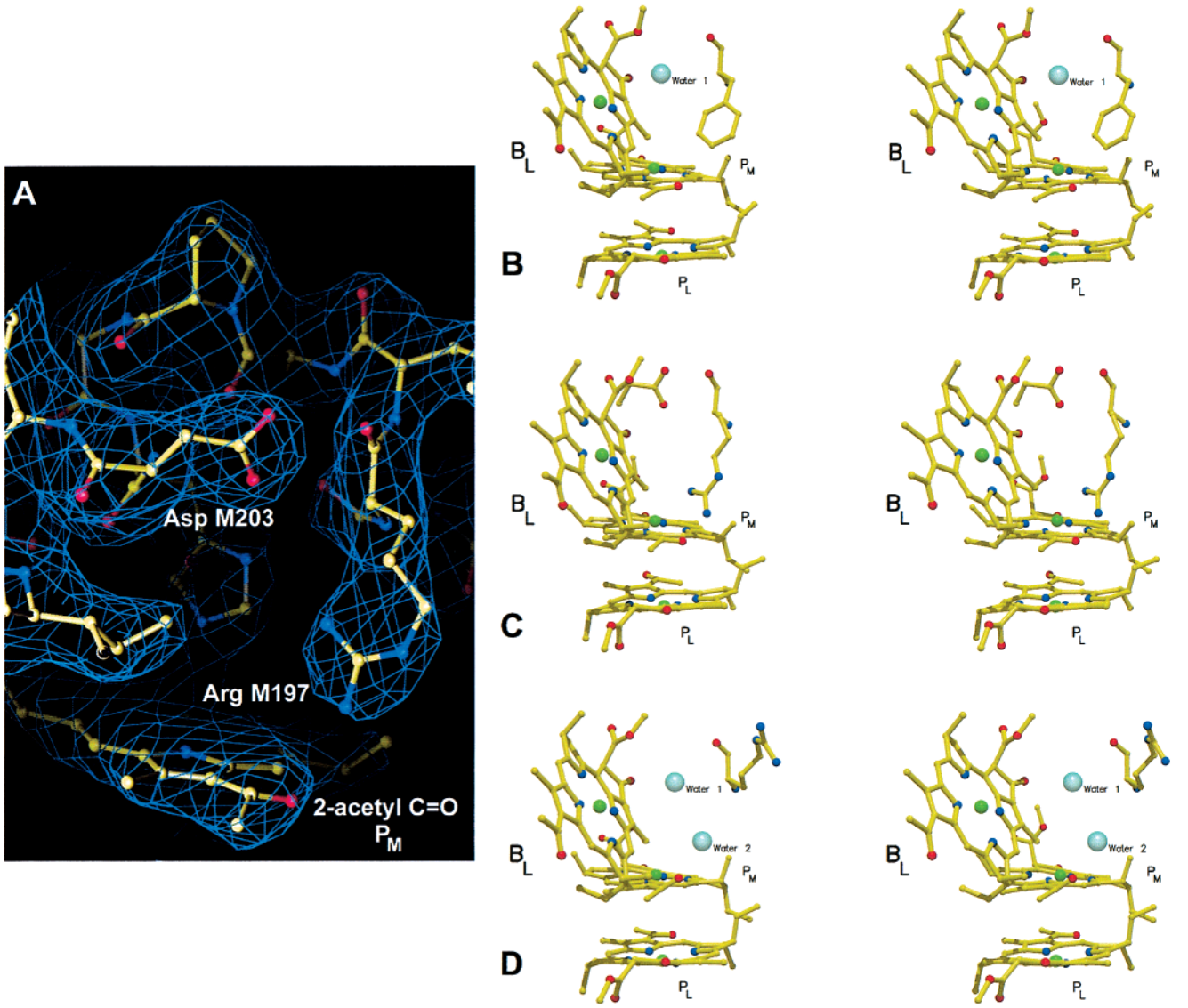

FIGURE 2: (A) REFMAC $2mF_o - DF_c$ electron density map showing the fitted model of Asp M203, Arg M197, and the 2-acetyl carbonyl group of the P_M Bchl. (B−D) Stereoviews of structural models showing (B) the positions of Phe M197 and a crystallographically defined water (labeled 1) in the wild-type reaction center, (C) the positions of Arg M197 and Asp M203 in the FM197R/GM203D reaction center, and (D) the positions of Arg M197, water 1, and a new water (labeled 2) in the FM197R/YM177F reaction center.

effect was to cause a 15 nm blue shift of the P Q_y band. In the double FM197R/GM203D mutant reaction center, an even greater blue shift of the P Q_y band was observed, which could not be attributed to a simple additive effect of the single mutations.

X-ray Crystallography. To investigate the structural basis for the altered absorbance properties of the FM197R/GM203D reaction center, and compare this with structural data obtained for the FM197R reaction center (*15*), reaction centers of the double mutant were purified and crystallized as described in Materials and Methods. The details of the data collection and refinement are given in Table 2. Diffraction data were collected that were 92.6% complete to a resolution of 2.7 Å, and the structural model was constructed as described in Materials and Methods.

Changes in the structure of the reaction center induced by the combination of the FM197R and GM203D mutations were confined to the vicinity of the accessory BChl B_L and the P BChls, with no long-range changes in the structure of the protein. The temperature factors for the atoms of the M197 and M203 residues were comparable to those of neighboring residues that had not undergone a change in position as a result of the mutation. These temperature factors were in the range expected for buried amino acids with a well-defined conformation. Figure 2A shows part of the electron density map for the region encompassing residues Asp M203 and Arg M197, with the fitted structures. The data reveal that Asp M203 points toward the peptide carbonyl of residue Arg M197. The Arg M197 residue does not adopt the flipped-out conformation observed in the structure of the FM197R single mutants (*15*), but rather adopts a buried conformation, occupying a volume similar to that occupied by Phe M197 in the structure of the wild-type reaction center. This arrangement was accompanied by some movement of the backbone of the M subunit in the region of residues M191−M200, which form a loop connecting the transmembrane D helix with the periplasmic cd helix.

The significance of this movement was analyzed by comparing the positions of the α-carbons of the protein backbone in the structural models of the FM197R/GM203D

reaction center and the wild-type reaction center (data not shown) using the program LSQKAB (*30*). The movement was greatest at Asn M195, where a 2.1 Å displacement of the α-carbon was found as compared with a root-mean-square α-carbon displacement of 0.48 Å for the entire model. There was no significant movement of the backbone of residue M203, which lies outside the loop region, forming part of the transmembrane D helix. Movement of the backbone in the M191−M200 loop region mainly affected the positions of residues Tyr M198, Leu M196, and Asn M195, which are exposed at the periplasmic surface of the protein, but did not bring about any major changes in the packing of these residues. The cause of this limited repacking of a small part of the M subunit is discussed below.

Packing of Residue Asp M203. Figure 2B shows a stereoview of the interface region between B_L and P_M/P_L in the wild-type reaction center, showing the positions of Phe M197 and a crystallographically defined water molecule that is within hydrogen bonding distance of the 9-keto carbonyl group of B_L. The question of whether this water molecule is in fact hydrogen bonded to this carbonyl group is considered in more detail below. A stereoview of the structural model of the same region in the FM197R/GM203D reaction center is shown in Figure 2C. As indicated above, the side chain of Asp M203 was found to be pointing toward the backbone carbonyl of Arg M197. One of the carboxy oxygens of Asp M203 takes up part of the volume occupied in the wild-type reaction center by the water (labeled 1) shown in Figure 2B, and the interpretation of the electron density maps is that the substitution of Asp for Gly at M203 causes exclusion of this water molecule from the complex. The possible role of this water molecule and the significance of its displacement is discussed below. The conformation adopted by the side chain of Arg M197 is similar to that adopted by Phe M197 in the wild-type reaction center (Figure 2, panel C compared with panel B), pointing toward the 2-acetyl carbonyl of P_M. This "buried" conformation was quite distinct from the flipped-out conformation seen in the structure of the FM197R single mutant (not shown) and in that of the FM197R/YM177F reaction center, which is shown for comparison in Figure 2D. In the FM197R and FM197R/YM177F reaction centers, the cavity created by the adoption of the flipped-out conformation by Arg M197 was partially filled by a water molecule, labeled 2 in Figure 2D.

Why Is the Packing of Residue Arg M197 Affected by the Presence of Asp M203? In the FM197R single mutant, the flipped-out conformation adopted by Arg M197 is facilitated by a cleft at the interface of the L and M subunits that extends to the periplasmic surface of the protein (*15*). The buried conformation adopted by this residue in the FM197R/GM203D reaction center was not caused by a closure of this cleft. In fact, due to the repacking of Tyr M198 and Asn M195 described above, this cleft is slightly wider in the FM197R/GM203D reaction center than in the wild-type reaction center or FM197R reaction center (data not shown).

Two alternative explanations have been considered in an attempt to account for the buried conformation adopted by Arg M197 when Asp M203 is also present. The first explanation is that the need to accommodate an Asp in place of Gly at the M203 position causes the observed change in the position of the backbone in the M191−M200 region, and that a consequence of this change in packing is that there is sufficient room to accommodate the longer Arg M197 residue in the buried position in place of the wild-type Phe residue. According to this explanation, steric constraints cause the Arg M197 residue to adopt the flipped-out conformation in the FM197R reaction center, but the loosening of the structure caused by the Gly to Asp mutation at the M203 position in the FM197R/GM203D reaction center overcomes these steric constraints, allowing Arg M197 to adopt the buried conformation.

A second possibility is that there is an interaction between Asp M203 and Arg M197 during folding of the double mutant protein, which limits the freedom of movement of the latter. In the case of the FM197R reaction center, a salt bridge interaction formed between Arg M197 and Asp L155 during folding of the protein was proposed as one explanation of why Arg M197 adopts the flipped-out conformation (*15*). In the FM197R/GM203D reaction center, a similar (and preferred) interaction between Arg M197 and Asp M203 could restrict the freedom of movement of Arg M197, leading to the buried conformation observed in the assembled FM197R/GM203D reaction center. This interaction would have to be broken before assembly of the protein is complete, as in the fully assembled complex Asp M203 interacts with the peptide carbonyl of Arg M197 and not the terminal amino groups. However, it may be possible that breakage of an interaction between the residues of Arg M197 and Asp M203 occurs at a point during the folding of the protein when it is no longer possible for Arg M197 to adopt the flipped-out conformation. In this case, the change in conformation of Arg M197 would be a consequence of introducing a nearby acidic residue, forming a favorable acid−base interaction. Repacking of the backbone of the M subunit in the M191−M200 region would then be attributable to the requirement to accommodate Arg M197 and/or Asp M203 in the observed conformations.

At present, we cannot distinguish between these possibilities, but one way forward would be to introduce a Gly to Leu mutation at position M203, as Leu is similar in shape and size to Asp, but could not form an ionic interaction with the side chain of Arg M197.

Possible Origins of the Blue Shift of the P Q_y Band. In our recent description of the X-ray crystal structure of the FM197R/YM177F reaction center, it was noted that the flipped-out conformation adopted by Arg M197 was accompanied by a marked (∼20°) out-of-plane rotation of the 2-acetyl carbonyl group of P_M (*15*). The C12−C2−C2a−O dihedral angle (ϕ_{Ac}) for P_M in the structural model of the FM197R/YM177F reaction center was 41°, the group sitting markedly out of the plane of the BChl ring. In marked contrast, ϕ_{Ac} for the P_M BChl in the structural model of the FM197R/GM203D reaction center was −7°, an almost in-plane geometry. In assigning this conformation, we have assumed, as in our previous study, that the oxygen "arm" of the acetyl group points toward the M197 residue. This would place one of the terminal nitrogens of Arg M197 approximately 2.4 Å from the keto oxygen of the 2-acetyl carbonyl of P_M, and thus in a suitable position to form a hydrogen bond. Taken together, these findings suggest that the cavity created when Arg M197 adopts the flipped-out conformation allows an out-of-plane rotation of the P_M 2-acetyl carbonyl group. Conversely, the change in packing that occurs when Arg M197 adopts the buried conformation

pushes the P_M 2-acetyl carbonyl group back into the plane of the ring (and in fact pushes the keto oxygen slightly below the plane of the ring).

In our report of the properties of the FM197R/YM177F reaction center, the possibility that the blue shift of the P Q_y band seen in this complex is attributable to the observed 20° out-of-plane rotation of the 2-acetyl carbonyl group of P_M was discussed (*15*). When introduced singly, the FM197R mutation causes a blue shift of the P Q_y band (relative to the position in the spectrum of the wild-type reaction center) of 13 nm at room temperature (*16*), 15 nm at 77 K (Figure 1), and 17 nm at 12 K (*17*). The FM197R/GM203D reaction center also exhibited a blue shift of the P Q_y band, the magnitude of which was more sensitive to temperature than in the case of the FM197R reaction center [13 nm at room temperature (*16*), 25 nm at 77 K (Figure 1), and 29 nm at 12 K (*17*)]. Given the details of the X-ray structure, the blue shift of the P Q_y band of the FM197R/GM203D reaction center cannot be attributed to a pronounced out-of-plane geometry of the P_M 2-acetyl carbonyl group.

The most obvious alternative explanation for this change in the absorbance spectrum is that a general loosening of the structure of the FM197R/GM203D reaction center causes a slight increase in the spacing of the BChls of the P dimer, which would decrease the excitonic coupling between the two halves of the dimer, resulting in an increase in the energy of the P Q_y band. It has been estimated that a 15 nm blue shift of the P Q_y band would require an increase in the separation of the two halves of the P BChl dimer of only 0.1 Å (*31*). This explanation does not disprove the hypothesis that the blue shift of the P Q_y band in the FM197R/YM177F reaction center is a consequence of the out-of-plane geometry of the P_M 2-acetyl carbonyl group however. There is no a priori reason to assume that the blue shift has the same structural origin in the two reaction centers, and the need for caution is highlighted by the observation of different conformations for Arg M197 in the two reaction centers. Likewise, there is no a priori reason to assume that a given change in spectrum has only one cause. If the blue shifts of the P Q_y band seen in the FM197R and FM197R/GM203D reaction centers have different structural origins, this could explain the apparent difference in the temperature dependence of the magnitude of the shift of the band in the two reaction centers. Clearly, this is a topic that requires further investigation, and crystallographic studies of other mutant reaction centers that show shifts of the P Q_y band are underway.

Another point to note is that the P Q_y band is not significantly blue shifted in the GM203D single mutant reaction center (Figure 1). If the blue shift of this band in the FM197R/GM203D reaction center is due to an increase in the interdimer spacing, this would suggest that the GM203D mutation alone does not cause the structural changes that lead to this increase in spacing. A possibility, therefore, is that this increase is caused by Arg M197 adopting the buried conformation.

Consequences of the Packing of Residue Asp M203. Due to its location, the GM203D mutation also affected the structure of the protein in the immediate vicinity of the 9-keto carbonyl group of the B_L BChl. In the X-ray crystal structures of the wild-type reaction center of both *Rb. sphaeroides* and *Rhodopseudomonas viridis*, this carbonyl group is within hydrogen-bonding distance of a water molecule (*6*, *7*, *32*), the position of which is shown in Figure 2B (a similar interaction is apparent for the 9-keto carbonyl group of the symmetry-related B_M BChl). In the structure of the FM197R/GM203D reaction center, this water molecule is absent, the volume normally occupied by this water molecule instead being occupied by one of the carboxyl oxygens of Asp M203 (Figure 2, panel C compared with panel B). This carbonyl oxygen is 3.7 Å from the oxygen of the 9-keto carbonyl of the B_L BChl. The geometry of the Asp is such that a hydrogen bond interaction with the 9-keto carbonyl of P_M is unlikely. In the wild-type reaction center, the water that is excluded by the GM203D mutation is also within hydrogen-bonding distance of residue His M202, which in turn provides the axial ligand for the P_M BChl. The position and conformation of His M202 were not affected by the exclusion of this water and the other changes in structure observed in the FM197R/GM203D reaction center.

Raman spectroscopy has also been used to study the interaction of the 9-keto carbonyl of B_L with the surrounding protein. In fact, the first suggestion that the 9-keto carbonyl of B_L is hydrogen bonded in the wild-type reaction center was made on the basis of Raman spectroscopy (*33*). By comparing the resonance Raman spectrum of the accessory BChls in the absence and presence of an oxidized primary donor, Robert and Lutz concluded that either the 9-keto carbonyl group of B_L is hydrogen bonded to the protein only when the P Bchls are oxidized or an existing, weak hydrogen bond is strengthened on oxidation of P (*33*). At the time of this study, no donor of a hydrogen bond was obvious from the available X-ray crystal structures of the *Rb. sphaeroides* reaction center, which did not contain modeled waters, and so Robert and Lutz (*33*) proposed that this hydrogen bond donor should be a water molecule. This proposal subsequently received support through the publication of improved structural models for the *Rps. viridis* and *Rb. sphaeroides* reaction centers that contain modeled waters (*6*, *7*), and was further developed through a discussion of how the P^+-induced change in hydrogen bonding is brought about (*37*, *38*). In particular, it was noted that the water concerned is also within hydrogen-bonding distance of His M202, which in turn provides the axial ligand to one of the BChls of P (*37*, *38*).

Recently, Czarnecki and co-workers (*20*) have pointed out that the stretching frequencies of the 9-keto carbonyl groups of B_L and B_M are similar to those obtained for this group in isolated BChl in a non-hydrogen-bonding solvent, and so have questioned whether the 9-keto carbonyl groups are in fact hydrogen bonded to the water molecules that are observed in the X-ray crystal structures. Using *Rb. capsulatus* reaction centers with the mutation Gly M201 to Asp (GM201D), which is equivalent to the *Rb. sphaeroides* GM203D mutation, Czarnecki and co-workers also made the observation that the Gly to Asp mutation causes a 7 cm^{-1} upshift of the stretching frequency of the 9-keto carbonyl of B_L (*20*). On the premise that this carbonyl group is not hydrogen bonded in the wild-type reaction center, this effect was attributed to a change in the environment of the 9-keto carbonyl group due to Asp M201 carrying a negative charge.

Our finding that the Gly to Asp mutation causes exclusion of a water that is located close to the 9-keto carbonyl of B_L provides alternative explanations for the destabilizing effect of this mutation on B_L^-. One possibility is that, by exclusion

of this water molecule, the mutation prevents a hydrogen bond interaction which would stabilize B_L^-, particularly when P is in the form P^+ (i.e., during charge separation). An alternative view is that the mutation affects the Raman spectrum of the B_L BChl through a change in the dielectric properties of the environment of the 9-keto carbonyl of B_L. This change includes both the replacement of a Gly with an Asp, and also the removal of a water located close to the 9-keto carbonyl group. The effects of changes in dielectric constant on the stretching frequency of carbonyl groups have been discussed previously (*36*).

Relevance of the Structural Data to the GM203D Single Mutant. Of obvious relevance to this discussion is the question of whether the structural changes in the immediate vicinity of the 9-keto carbonyl of the B_L BChl, observed in the crystal structure of the FM197R/GM203D double mutant, are also likely to have taken place in the GM203D single mutant. In the absence of crystallographic data on the latter, it is not possible to be certain that Asp M203 also displaces the relevant water molecule in the single GM203D mutant reaction center (or for that matter in the GM201D and GM201D/LM212H mutants of *Rb. capsulatus*). However, from a comparison of the structures of the wild-type and FM197R/GM203D reaction centers, this seems likely to be the case. In the wild-type complex, the distance from the CA of Gly M203 to the hydrogen-bonding water is only 3.3 Å, while the distance from the CA of Gly M203 to the oxygen atom of the 9-keto carbonyl group of B_L is only 3.5 Å (distances taken from the structural model published in ref *15*). The close proximity of these atoms makes it very difficult to envisage how the Gly at M203 could be changed to Asp without causing a displacement of the water molecule, unless some large-scale structural rearrangement of the protein is invoked. Likewise, in the structural model of the FM197R/GM203D reaction center, it is difficult to see how both the Asp M203 residue and the water molecule could be included in the structure without again undergoing some larger-scale structural rearrangements. Our conclusion, therefore, is that the changes in structure in the vicinity of the 9-keto carbonyl of the B_L BChl observed for the FM197R/GM203D reaction center are also likely to have occurred in the single GM203D reaction center. More consideration is given to this point below.

Consequences of the GM203D Mutation for the Energetics of Electron Transfer. The mutation Gly M203 to Asp was originally designed with a view of adding a hydrogen bond to the 9-keto carbonyl group of the B_L BChl (*18*). At the time that the mutation was first reported, the available X-ray crystal structures of the reaction center did not include water molecules. By analogy with well-documented effects of hydrogen bonding on the redox properties of P (*37*, *38*), the addition of a hydrogen bond would be expected to make B_L easier to reduce, lowering the free energy of the $P^+B_L^-$ state. The GM203D mutation was of particular interest in light of the controversy over the role of the $P^+B_L^-$ state during electron transfer from P* to H_L, which stemmed mainly from the fact that it is very difficult to resolve a discrete $P^+B_L^-$ state in transient absorption experiments. There is now an increasing amount of evidence that the $P^+B_L^-$ state does form as a discrete intermediate (*11*−*14*), but only at a low level because the reaction $P^+B_L^- \rightarrow P^+H_L^-$ is approximately twice as rapid as the preceding reaction $P^* \rightarrow P^+B_L^-$. On analysis, the GM203D mutation was found to bring about a 3-fold decrease in the rate of P* decay (*18*). The explanation offered for this effect was that the free energy gap between P* and $P^+B_L^-$ is optimized in the wild-type reaction center (*18*) and that the mutation stabilizes B_L^-, increasing this free energy gap and placing the energetics of the reaction in the Marcus inverted region, where increases in the driving force for a reaction bring about a decrease in the rate. As discussed above, recently Czarnecki and co-workers have proposed that the amino acid equivalent to Asp M203 in the *Rb. capsulatus* GM201D reaction center is charged, and so destabilizes the B_L^- anion, raising the free energy of the $P^+B_L^-$ state and slowing primary electron transfer (*20*).

The finding reported in this study, that the GM203D mutation causes exclusion of a crystallographically defined water molecule and so removes the possibility of a hydrogen bond interaction with the 9-keto carbonyl group, provides an alternative explanation for the electron transfer properties of the GM203D reaction center. Abolition of a weak hydrogen bond (which may only be present when P is oxidized) would be expected to increase the free energy of the $P^+B_L^-$ state, and cause the observed slowing of primary electron transfer. An increase in the free energy of the $P^+B_L^-$ state through an effect on the redox properties of B_L (but not on the redox properties of P) would also bring this state closer in energy to the equivalent state $P^+B_M^-$ on the inactive cofactor branch, which is thought to lie at a higher energy than the $P^+B_L^-$ state. This would help to explain why limited inactive branch electron transfer is seen in *Rb. capsulatus* reaction centers with the LM212H (β) mutation when the GM201D mutation is added as a second change (*19*). Finally, the observed upshift of the stretching frequency of the 9-keto carbonyl group of B_L that accompanies the GM201D mutation in the *Rb. capsulatus* reaction center (*20*) is consistent with the expected effect of the breakage of a weak hydrogen bond, or alternatively a change in the dielectric properties of the environment of this group, caused by exclusion of the adjacent water.

ACKNOWLEDGMENT

We thank HASYLAB/DESY for the use of synchrotron facilities and staff at the EMBL BW7B beamline for assistance with data collection.

REFERENCES

1. Allen, J. P., Feher, G., Yeates, T. O., Rees, D. C., Deisenhofer, J., Michel, H., and Huber, R. (1986) *Proc. Natl. Acad. Sci. U.S.A. 83*, 8589−8593.
2. Allen, J. P., Feher, G., Yeates, T. O., Komiya, H., and Rees, D. C. (1987) *Proc. Natl. Acad. Sci. U.S.A. 84*, 5730−5734.
3. Komiya, H., Yeates, T. O., Rees, D. C., Allen, J. P., and Feher, G. (1988) *Proc. Natl. Acad. Sci. U.S.A. 85*, 9012−9016.
4. Chang, C.-H., Tiede, D., Tang, J., Smith, U., Norris, J., and Schiffer, M. (1986) *FEBS Lett. 205*, 82−86.
5. Chang, C.-H., El-Kabbani, O., Tiede, D., Norris, J., and Schiffer, M. (1991) *Biochemistry 30*, 5352−5360.
6. Ermler, U., Fritzsch, G., Buchanan, S. K., and Michel, H. (1994) *Structure 2*, 925−936.
7. Ermler, U., Michel, H., and Schiffer, M. (1994) *J. Bioenerg. Biomembr. 26*, 5−15.
8. Parson, W. W. (1991) in *Chlorophylls* (Scheer, H., Ed.) pp 1153−1180, CRC Press, Boca Raton, FL.
9. Fleming, G. R., and van Grondelle, R. (1994) *Phys. Today 47*, 48−55.

10. Hoff, A. J., and Deisenhofer, J. (1997) *Phys. Lett. 287*, 2−247.
11. Arlt, T., Schmidt, S., Kaiser, W., Lauterwasser, C., Meyer, M., Scheer, H., and Zinth, W. (1993) *Proc. Natl. Acad. Sci. U.S.A. 90*, 11757−11761.
12. van Stokkum, I. H. M., Beekman, L. M. P., Jones, M. R., van Brederode, M. E., and van Grondelle, R. (1997) *Biochemistry 36*, 11360−11368.
13. Holzwarth, A. R., and Müller, M. G. (1996) *Biochemistry 35*, 11820−11831.
14. Arlt, T., Bibikova, M., Penzkofer, H., Oesterhelt, D., and Zinth, W. (1996) *J. Phys. Chem. 100*, 12060−12065.
15. McAuley-Hecht, K. E., Fyfe, P. K., Ridge, J. P., Prince, S. M., Hunter, C. N., Isaacs, N. W., Cogdell, R. J., and Jones, M. R. (1998) *Biochemistry 37*, 4740−4750.
16. Ridge, J. P. (1998) Ph.D. Thesis, University of Sheffield, Sheffield, United Kingdom.
17. Vos, M. H., Rischel, C., Breton, J., Martin, J.-L., Ridge, J. P., and Jones, M. R. (1998) *Photosynth. Res. 55*, 181−187.
18. Williams, J. C., Alden, R. G., Murchison, H. A., Peloquin, J. M., Woodbury, N. W., and Allen, J. P. (1992) *Biochemistry 31*, 11029−11037.
19. Heller, B. A., Holten, D., and Kirmaier, C. (1995) *Science 269*, 940−945.
20. Czarnecki, K., Kirmaier, C., Holten, D., and Bocian, D. F. (1999) *J. Phys. Chem. A 103*, 2235−2246.
21. Fyfe, P. K. (1997) Ph.D. Thesis, University of Glasgow, Glasgow, United Kingdom.
22. Fyfe, P. K., McAuley-Hecht, K. E., Ridge, J. P., Prince, S. M., Isaacs, N. W., Cogdell, R. J., and Jones, M. R. (1998) *Photosynth. Res. 55*, 133−140.
23. Otwinowski, Z., and Minor, W. (1997) *Methods Enzymol. 276*, 307−326.
24. Brünger, A. T., Kuriyan, J., and Karplus, M. (1987) *Science 235*, 458−460.
25. Jones, T. A., Zou, J. Y., Cowan, S. W., and Kjeldgaard, M. (1991) *Acta Crystallogr. A47*, 110−119.
26. Murshudov, G. N., Vagin A. A., and Dodson, E. J. (1997) *Acta Crystallogr. D53*, 240−255.
27. Kraulis, P. J. (1991) *J. Appl. Crystallogr. 24*, 946−950.
28. Merritt, E. A., and Bacon, D. J. (1997) *Methods Enzymol. 277*, 505−524.
29. McGlynn, P., Hunter, C. N., and Jones, M. R. (1994) *FEBS Lett. 349*, 349−353.
30. Kabsch, W. (1976) *Acta Crystallogr. A32*, 922−923.
31. Parson, W. W., and Warshel, A. (1987) *J. Am. Chem. Soc. 109*, 6152−6163.
32. Deisenhofer, J., Epp, O., Sinning, I., and Michel, H. (1995) *J. Mol. Biol. 246*, 429−457.
33. Robert, B., and Lutz, M. (1988) *Biochemistry 27*, 5108−5114.
34. Robert, B. (1990) *Biochim. Biophys. Acta 1017*, 99−111.
35. Robert, B. (1996) in *Biophysical Techniques in Photosynthesis* (Amesz, J., and Hoff, A. J., Eds.) pp 161−176, Kluwer Academic Publishers, Dordrecht, The Netherlands.
36. Krawczyk, S. (1989) *Biochim. Biophys. Acta 976*, 140−149.
37. Allen, J. P., and Williams, J. C. (1995) *J. Bioenerg. Biomembr. 27*, 275−283.
38. Ivancich, A., Artz, K., Williams, J. C., Allen, J. P., and Mattioli, T. A. (1998) *Biochemistry 37*, 11812−11820.
39. Brünger, A. T. (1992) *Nature 335*, 472−475.
40. Hooft, R. W. W., Vriend, G., Sander, C., and Abola, E. E. (1996) *Nature 381*, 272.
41. Laskowski, R. A., MacArthur, W. W., Moss, D. S., and Thornton, J. M. (1993) *J. Appl. Crystallogr. 26*, 283−291.
42. Cruickshank, D. W. J. (1999) *Acta Crystallogr. D55*, 583−601.

BI9925017